

# Real-Parameter Black-Box Optimization Benchmarking 2009: Noiseless Functions Definitions

Nikolaus Hansen, Steffen Finck, Raymond Ros, Anne Auger

► **To cite this version:**

Nikolaus Hansen, Steffen Finck, Raymond Ros, Anne Auger. Real-Parameter Black-Box Optimization Benchmarking 2009: Noiseless Functions Definitions. [Research Report] RR-6829, INRIA. 2009. <inria-00362633>

**HAL Id: inria-00362633**

**<https://hal.inria.fr/inria-00362633>**

Submitted on 18 Feb 2009

**HAL** is a multi-disciplinary open access archive for the deposit and dissemination of scientific research documents, whether they are published or not. The documents may come from teaching and research institutions in France or abroad, or from public or private research centers.

L'archive ouverte pluridisciplinaire **HAL**, est destinée au dépôt et à la diffusion de documents scientifiques de niveau recherche, publiés ou non, émanant des établissements d'enseignement et de recherche français ou étrangers, des laboratoires publics ou privés.

INSTITUT NATIONAL DE RECHERCHE EN INFORMATIQUE ET EN AUTOMATIQUE

***Real-Parameter Black-Box Optimization  
Benchmarking 2009: Noiseless Functions  
Definitions***

Nikolaus Hansen — Steffen Finck — Raymond Ros — Anne Auger

**N° 6829**

February 2009

Thème COG



*R*  
**apport  
de recherche**

ISSN INRIA/RR--6829--FR+ENG

ISSN 0249-6399



## Real-Parameter Black-Box Optimization Benchmarking 2009: Noiseless Functions Definitions

Nikolaus Hansen\*, Steffen Finck†, Raymond Ros‡, Anne Auger§

Thème COG — Systèmes cognitifs  
Équipes-Projets Adaptive Combinatorial Search et TAO

Rapport de recherche n° 6829 — February 2009 — 14 pages

**Abstract:** Quantifying and comparing performance of optimization algorithms is one important aspect of research in search and optimization. However, this task turns out to be tedious and difficult to realize even in the single-objective case – at least if one is willing to accomplish it in a scientifically decent and rigorous way. The BBOB 2009 workshop will furnish most of this tedious task for its participants: (1) choice and implementation of a well-motivated real-parameter benchmark function testbed, (2) design of an experimental set-up, (3) generation of data output for (4) post-processing and presentation of the results in graphs and tables. What remains to be done for the participants is to allocate CPU-time, run their favorite black-box real-parameter optimizer in a few dimensions a few hundreds of times and execute the provided post-processing script afterwards. In this report, the testbed of noise-free functions is defined and motivated.

**Key-words:** optimization, evolutionary algorithms, benchmarking, black-box

\* NH is with the Microsoft Research–INRIA Joint Centre, 28 rue Jean Rostand, 91893 Orsay Cedex, France

† SF is with the Research Center PPE, University of Applied Science Vorarlberg, Hochschulstrasse 1, 6850 Dornbirn, Austria

‡ RR is with the Univ. Paris-Sud, LRI, UMR 8623 / INRIA Saclay, projet TAO, F-91405 Orsay, France.

§ AA is with the TAO Team, INRIA Saclay, Université Paris Sud, LRI, 91405 Orsay cedex, France

## No French Title

**Résumé :** Pas de résumé

**Mots-clés :** Pas de motclef

## Contents

<b>0</b>	<b>Introduction</b>	<b>4</b>
0.1	General Setup . . . . .	4
	Search Space . . . . .	4
	Location of the optimal $\mathbf{x}^{\text{opt}}$ and of $f_{\text{opt}} = f(\mathbf{x}^{\text{opt}})$ . . . . .	4
	Boundary Handling . . . . .	5
	Linear Transformations . . . . .	5
	Non-Linear Transformations and Symmetry Breaking . . . . .	5
0.2	Symbols and Definitions . . . . .	5
<b>1</b>	<b>Separable functions</b>	<b>6</b>
1.1	Sphere Function . . . . .	6
	Properties . . . . .	6
1.2	Ellipsoidal Function . . . . .	6
	Properties . . . . .	7
1.3	Rastrigin Function . . . . .	7
	Properties . . . . .	7
1.4	Büche-Rastrigin Function . . . . .	7
	Properties . . . . .	7
1.5	Linear Slope . . . . .	7
	Properties . . . . .	7
<b>2</b>	<b>Functions with low or moderate conditioning</b>	<b>8</b>
2.6	Attractive Sector Function . . . . .	8
	Properties . . . . .	8
2.7	Step Ellipsoidal Function . . . . .	8
	Properties . . . . .	8
2.8	Rosenbrock Function, original . . . . .	8
	Properties . . . . .	8
2.9	Rosenbrock Function, rotated . . . . .	9
	Properties . . . . .	9
<b>3</b>	<b>Functions with high conditioning and unimodal</b>	<b>9</b>
3.10	Ellipsoidal Function . . . . .	9
	Properties . . . . .	9
3.11	Discus Function . . . . .	9
	Properties . . . . .	9
3.12	Bent Cigar Function . . . . .	9
	Properties . . . . .	9
3.13	Sharp Ridge Function . . . . .	10
	Properties . . . . .	10
3.14	Different Powers Function . . . . .	10
	Properties . . . . .	10
<b>4</b>	<b>Multi-modal functions with adequate global structure</b>	<b>10</b>
4.15	Rastrigin Function . . . . .	10
	Properties . . . . .	10
4.16	Weierstrass Function . . . . .	10
	Properties . . . . .	11
4.17	Schaffers F7 Function . . . . .	11
	Properties . . . . .	11
4.18	Schaffers F7 Function, moderately ill-conditioned . . . . .	11
	Properties . . . . .	11

4.19 Composite Griewank-Rosenbrock Function F8F2 . . . . .	11
Properties . . . . .	11
<b>5 Multi-modal functions with weak global structure</b>	<b>12</b>
5.20 Schwefel Function . . . . .	12
Properties . . . . .	12
5.21 Gallagher’s Gaussian 101-me Peaks Function . . . . .	12
Properties . . . . .	12
5.22 Gallagher’s Gaussian 21-hi Peaks Function . . . . .	12
Properties . . . . .	13
5.23 Katsuura Function . . . . .	13
Properties . . . . .	13
5.24 Lunacek bi-Rastrigin Function . . . . .	13
Properties . . . . .	13
<b>A Function Properties</b>	<b>14</b>
A.1 Deceptive Functions . . . . .	14
A.2 Ill-Conditioning . . . . .	14
A.3 Regularity . . . . .	14
A.4 Separability . . . . .	14
A.5 Symmetry . . . . .	14
A.6 Target function value to reach . . . . .	14

## 0 Introduction

In the following, 24 noise-free real-parameter single-objective benchmark functions are defined (for a graphical presentation see [1]). Our intention behind the selection of benchmark functions was to evaluate the performance of algorithms with regard to typical difficulties which we believe occur in continuous domain search. We hope that the function collection reflects, at least to a certain extent and with a few exceptions, a more difficult portion of the problem distribution that will be seen in practice (easy functions are evidently of lesser interest).

We prefer benchmark functions that are comprehensible such that algorithm behaviours can be understood in the topological context. In this way, a desired search behaviour can be pictured and deficiencies of algorithms can be profoundly analysed. Last but not least, this can eventually lead to a systematic improvement of algorithms.

All benchmark functions are scalable with the dimension. Most functions have no specific value of their optimal solution (they are randomly shifted in  $x$ -space). All functions have an artificially chosen optimal function value (they are randomly shifted in  $f$ -space). Consequently, for each function different *instances* can be generated: for each instance the randomly chosen values are drawn anew<sup>1</sup>. Apart from the first subgroup, the benchmarks are non-separable. Other specific properties are discussed in the appendix.

### 0.1 General Setup

**Search Space** All functions are defined and can be evaluated over  $\mathcal{R}^D$ , while the actual search domain is given as  $[-5, 5]^D$ .

**Location of the optimal  $\mathbf{x}^{\text{opt}}$  and of  $f_{\text{opt}} = f(\mathbf{x}^{\text{opt}})$**  All functions have their global optimum in  $[-5, 5]^D$ . The majority of functions has the global optimum in  $[-4, 4]^D$  and for many of them  $\mathbf{x}^{\text{opt}}$  is drawn uniformly from this compact. The value for  $f_{\text{opt}}$  is drawn from a Cauchy distributed random variable, with zero median and with roughly 50% of the values between -100 and 100.

<sup>1</sup>The implementation provides an instance ID as input, such that a set of uniquely specified instances can be explicitly chosen.

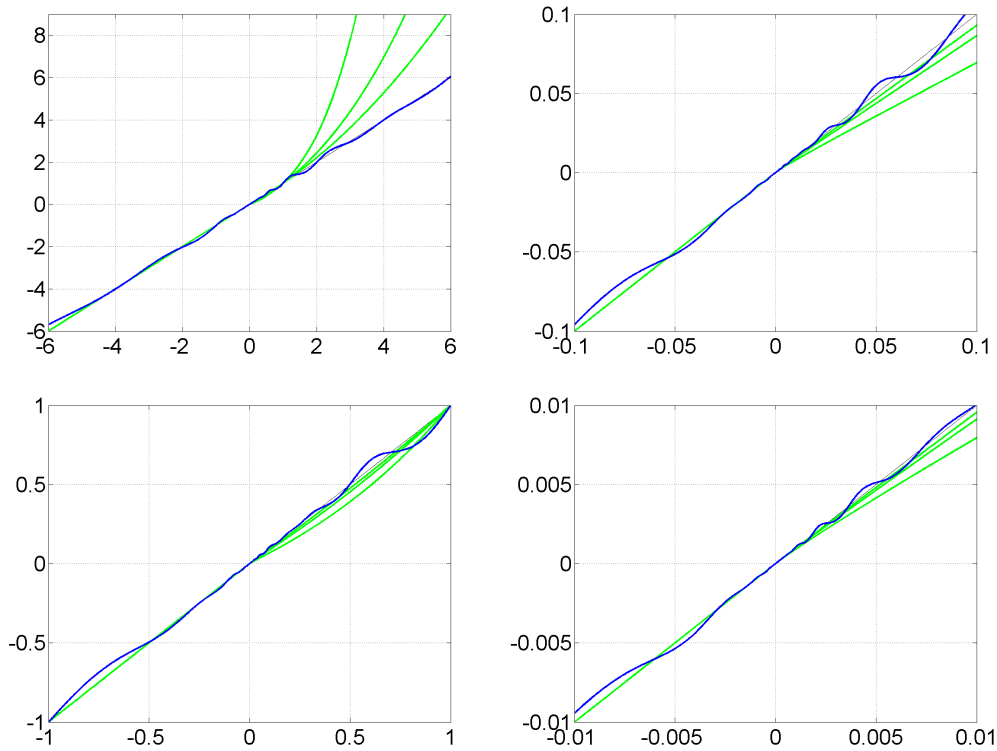


Figure 1:  $T_{osz}$  (blue) and  $D$ -th coordinate of  $T_{asy}$  for  $\beta = 0.1, 0.2, 0.5$  (green)

The value is rounded after two decimal places and set to  $\pm 1000$  if its absolute value exceeds 1000. In the function definitions a transformed variable vector  $\mathbf{z}$  is often used instead of the argument  $\mathbf{x}$ . The vector  $\mathbf{z}$  has its optimum in  $\mathbf{z}^{opt} = \mathbf{0}$ , if not stated otherwise.

**Boundary Handling** On some functions a penalty boundary handling is applied as given with  $f_{pen}$  (see next section).

**Linear Transformations** Linear transformations of the search space are applied to derive non-separable functions from separable ones and to control the conditioning of the function.

**Non-Linear Transformations and Symmetry Breaking** In order to make relatively simple, but well understood functions less regular, on some functions non-linear transformations are applied in  $x$ - or  $f$ -space. Both transformations  $T_{osz} : \mathcal{R}^n \rightarrow \mathcal{R}^n$  and  $T_{asy} : \mathcal{R}^D \rightarrow \mathcal{R}^D$  are defined coordinate-wise (see below). They are smooth and have, coordinate-wise, a strictly positive derivative. They are shown in Figure 1.  $T_{osz}$  is oscillating about the identity, where the oscillation is scale invariant w.r.t. the origin.  $T_{asy}$  is the identity for negative values. When  $T_{asy}$  is applied, a portion of  $1/2^D$  of the search space remains untransformed.

## 0.2 Symbols and Definitions

Used symbols and definitions of, e.g., auxiliary functions are given in the following. Vectors are typeset in bold and refer to column vectors.

$\otimes$  indicates element-wise multiplication of two  $D$ -dimensional vectors,  $\otimes : \mathcal{R}^D \times \mathcal{R}^D \rightarrow \mathcal{R}^D$ ,  $(\mathbf{x}, \mathbf{y}) \mapsto \text{diag}(\mathbf{x}) \times \mathbf{y} = (x_i \times y_i)_{i=1, \dots, D}$



$\|\cdot\|$  denotes the Euclidean norm,  $\|\mathbf{x}\|^2 = \sum_i x_i^2$ .

$[\cdot]$  denotes the nearest integer value

$\mathbf{0} = (0, \dots, 0)^T$  all zero vector

$\mathbf{1} = (1, \dots, 1)^T$  all one vector

$\Lambda^\alpha$  is a diagonal matrix in  $D$  dimensions with the  $i$ th diagonal element as  $\lambda_{ii} = \alpha^{\frac{1}{2} \frac{i-1}{D-1}}$ , for  $i = 1, \dots, D$ .

$f_{\text{pen}} : \mathcal{R}^D \rightarrow \mathcal{R}$ ,  $\mathbf{x} \mapsto \sum_{i=1}^D \max(0, |x_i| - 5)^2$

$\mathbf{1}_\pm^+$  a  $D$ -dimensional vector with entries of  $-1$  or  $1$  with equal probability independently drawn.

$\mathbf{Q}, \mathbf{R}$  orthogonal (rotation) matrices. For one function in one dimension a different realization for respectively  $\mathbf{Q}$  and  $\mathbf{R}$  is used for each instantiation of the function. Orthogonal matrices are generated from standard normally distributed entries by Gram-Schmidt orthonormalization. Columns and rows of an orthogonal matrix form an orthonormal basis.

$\mathbf{R}$  see  $\mathbf{Q}$

$T_{\text{asy}}^\beta : \mathcal{R}^D \rightarrow \mathcal{R}^D$ ,  $x_i \mapsto \begin{cases} x_i^{1+\beta \frac{i-1}{D-1} \sqrt{x_i}} & \text{if } x_i > 0 \\ x_i & \text{otherwise} \end{cases}$ , for  $i = 1, \dots, D$ . See Figure 1.

$T_{\text{osz}} : \mathcal{R}^n \rightarrow \mathcal{R}^n$ , for any positive integer  $n$  ( $n = 1$  and  $n = D$  are used in the following), maps element-wise

$$x \mapsto \text{sign}(x) \exp(\hat{x} + 0.049(\sin(c_1 \hat{x}) + \sin(c_2 \hat{x})))$$

with  $\hat{x} = \begin{cases} \log(|x|) & \text{if } x \neq 0 \\ 0 & \text{otherwise} \end{cases}$ ,  $\text{sign}(x) = \begin{cases} -1 & \text{if } x < 0 \\ 0 & \text{if } x = 0 \\ 1 & \text{otherwise} \end{cases}$ ,  $c_1 = \begin{cases} 10 & \text{if } x > 0 \\ 5.5 & \text{otherwise} \end{cases}$  and

$c_2 = \begin{cases} 7.9 & \text{if } x > 0 \\ 3.1 & \text{otherwise} \end{cases}$ . See Figure 1.

$\mathbf{x}^{\text{opt}}$  optimal solution vector, such that  $f(\mathbf{x}^{\text{opt}})$  is minimal.

## 1 Separable functions

### 1.1 Sphere Function

$$f_1(\mathbf{x}) = \|\mathbf{z}\|^2 + f_{\text{opt}} \quad (1)$$

- $\mathbf{z} = \mathbf{x} - \mathbf{x}^{\text{opt}}$

**Properties** Presumably the most easy continuous domain search problem, given the volume of the searched solution is small (i.e. where pure monte-carlo random search is too expensive).

- unimodal
- highly symmetric, in particular rotationally invariant

### 1.2 Ellipsoidal Function

$$f_2(\mathbf{x}) = \sum_{i=1}^D 10^{6 \frac{i-1}{D-1}} z_i^2 + f_{\text{opt}} \quad (2)$$

- $\mathbf{z} = T_{\text{osz}}(\mathbf{x} - \mathbf{x}^{\text{opt}})$

**Properties** Globally quadratic and ill-conditioned function with smooth local irregularities.

- unimodal
- conditioning is about  $10^6$

### 1.3 Rastrigin Function

$$f_3(\mathbf{x}) = 10 \left( D - \sum_{i=1}^D \cos(2\pi z_i) \right) + \|\mathbf{z}\|^2 + f_{\text{opt}} \quad (3)$$

- $\mathbf{z} = \Lambda^{10} T_{\text{asy}}^{0.2}(T_{\text{osz}}(\mathbf{x} - \mathbf{x}^{\text{opt}}))$

**Properties** Highly multimodal function with a comparatively regular structure for the placement of the optima. The transformations  $T_{\text{asy}}$  and  $T_{\text{osz}}$  alleviate the symmetry and regularity of the original Rastrigin function

- roughly  $10^D$  local optima
- conditioning is about 10

### 1.4 Büche-Rastrigin Function

$$f_4(\mathbf{x}) = 10 \left( D - \sum_{i=1}^D \cos(2\pi z_i) \right) + \sum_{i=1}^D z_i^2 + 100 f_{\text{pen}}(\mathbf{x}) + f_{\text{opt}} \quad (4)$$

- $z_i = s_i T_{\text{osz}}(x_i - x_i^{\text{opt}})$  for  $i = 1 \dots D$
- $s_i = \begin{cases} 10 \times 10^{\frac{1}{2} \frac{i-1}{D-1}} & \text{if } z_i > 0 \text{ and } i = 1, 3, 5, \dots \\ 10^{\frac{1}{2} \frac{i-1}{D-1}} & \text{otherwise} \end{cases}$  for  $i = 1, \dots, D$

**Properties** Highly multimodal function with a structured but highly asymmetric placement of the optima. Constructed as a deceptive function for symmetrically distributed search operators.

- roughly  $10^D$  local optima
- conditioning is about 10
- skew factor is about 10 in  $x$ -space and 100 in  $f$ -space

### 1.5 Linear Slope

$$f_5(\mathbf{x}) = \sum_{i=1}^D 5 |s_i| - s_i z_i + f_{\text{opt}} \quad (5)$$

- $z_i = x_i$  if  $x_i^{\text{opt}} x_i < 5^2$  and  $z_i = x_i^{\text{opt}}$  otherwise, for  $i = 1, \dots, D$ . That is, if  $x_i$  exceeds  $x_i^{\text{opt}}$  it will be mapped back into the domain and the function appears to be constant in this direction.
- $s_i = \text{sign}(x_i^{\text{opt}}) 10^{\frac{i-1}{D-1}}$  for  $i = 1, \dots, D$ .
- $\mathbf{x}^{\text{opt}} = \mathbf{z}^{\text{opt}} = 5 \times \mathbf{1}_{\pm}^+$

**Properties** Purely linear function testing whether the search can go outside the initial convex hull of solutions right into the domain boundary.

- $\mathbf{x}^{\text{opt}}$  is on the domain boundary

## 2 Functions with low or moderate conditioning

### 2.6 Attractive Sector Function

$$f_6(\mathbf{x}) = T_{\text{osz}} \left( \sum_{i=1}^D (s_i z_i)^2 \right)^{0.9} + f_{\text{opt}} \quad (6)$$

- $\mathbf{z} = \mathbf{Q}\Lambda^{10}\mathbf{R}(\mathbf{x} - \mathbf{x}^{\text{opt}})$
- $s_i = \begin{cases} 10^2 & \text{if } z_i > 0 \\ 1 & \text{otherwise} \end{cases}$

**Properties** Highly asymmetric function, where only one “hypercone” (with angular base area) with a volume of roughly  $1/2^D$  yields low function values. The optimum is located at the tip of this cone.

- unimodal

### 2.7 Step Ellipsoidal Function

$$f_7(\mathbf{x}) = 0.1 \max \left( |\hat{z}_1|/10^4, \sum_{i=1}^D 10^{2\frac{i-1}{D-1}} z_i^2 \right) + f_{\text{pen}}(\mathbf{x}) + f_{\text{opt}} \quad (7)$$

- $\hat{\mathbf{z}} = \Lambda^{10}\mathbf{R}(\mathbf{x} - \mathbf{x}^{\text{opt}})$
- $\tilde{z}_i = \begin{cases} \lfloor 0.5 + \hat{z}_i \rfloor & \text{if } \hat{z}_i > 0.5 \\ \lfloor 0.5 + 10 \hat{z}_i \rfloor / 10 & \text{otherwise} \end{cases}$  for  $i = 1, \dots, D$ ,  
denotes the rounding procedure in order to produce the plateaus.
- $\mathbf{z} = \mathbf{Q}\tilde{\mathbf{z}}$

**Properties** The function consists of many plateaus of different sizes. Apart from a small area close to the global optimum, the gradient is zero almost everywhere.

- conditioning is about 100

### 2.8 Rosenbrock Function, original

$$f_8(\mathbf{x}) = \sum_{i=1}^{D-1} \left( 100 (z_i^2 - z_{i+1})^2 + (z_i - 1)^2 \right) + f_{\text{opt}} \quad (8)$$

- $\mathbf{z} = \max \left( 1, \frac{\sqrt{D}}{8} \right) (\mathbf{x} - \mathbf{x}^{\text{opt}}) + 1$
- $\mathbf{z}^{\text{opt}} = \mathbf{1}$

**Properties** So-called banana function due to its 2-D contour lines as a bent ridge (or valley). In the beginning, the prominent first term of the function definition attracts to the point  $\mathbf{z} = \mathbf{0}$ . Then, a long bending valley needs to be followed to reach the global optimum. The ridge changes its orientation  $D - 1$  times.

- a local optimum with an attraction volume of about 25%

## 2.9 Rosenbrock Function, rotated

$$f_9(\mathbf{x}) = \sum_{i=1}^{D-1} \left( 100 (z_i^2 - z_{i+1})^2 + (z_i - 1)^2 \right) + f_{\text{opt}} \quad (9)$$

- $\mathbf{z} = \max \left( 1, \frac{\sqrt{D}}{8} \right) \mathbf{R}\mathbf{x} + \mathbf{1}/2$
- $\mathbf{z}^{\text{opt}} = \mathbf{1}$

**Properties** rotated version of the previously defined Rosenbrock function

## 3 Functions with high conditioning and unimodal

### 3.10 Ellipsoidal Function

$$f_{10}(\mathbf{x}) = \sum_{i=1}^D 10^{6 \frac{i-1}{D-1}} z_i^2 + f_{\text{opt}} \quad (10)$$

- $\mathbf{z} = T_{\text{osz}}(\mathbf{R}(\mathbf{x} - \mathbf{x}^{\text{opt}}))$

**Properties** Globally quadratic ill-conditioned function with smooth local irregularities, non-separable counterpart to  $f_2$ .

- conditioning is  $10^6$

### 3.11 Discus Function

$$f_{11}(\mathbf{x}) = 10^6 z_1^2 + \sum_{i=2}^D z_i^2 + f_{\text{opt}} \quad (11)$$

- $\mathbf{z} = T_{\text{osz}}(\mathbf{R}(\mathbf{x} - \mathbf{x}^{\text{opt}}))$

**Properties** Globally quadratic function with local irregularities. A single direction in search space is a thousand times more sensitive than all others.

- conditioning is about  $10^6$

### 3.12 Bent Cigar Function

$$f_{12}(\mathbf{x}) = z_1^2 + 10^6 \sum_{i=2}^D z_i^2 + f_{\text{opt}} \quad (12)$$

- $\mathbf{z} = \mathbf{R} T_{\text{asy}}^{0.5}(\mathbf{R}(\mathbf{x} - \mathbf{x}^{\text{opt}}))$

**Properties** A smooth but very narrow ridge needs to be followed. Due to  $T_{\text{asy}}^{1/2}$  the overall shape deviates remarkably from being quadratic.

- conditioning is about  $10^6$

### 3.13 Sharp Ridge Function

$$f_{13}(\mathbf{x}) = z_1^2 + 100 \sqrt{\sum_{i=2}^D z_i^2} + f_{\text{opt}} \quad (13)$$

- $\mathbf{z} = \mathbf{Q}\Lambda^{10}\mathbf{R}(\mathbf{x} - \mathbf{x}^{\text{opt}})$

**Properties** In this sharp ridge topology, the gradient is independent of the distance to the ridge. Approaching the ridge is initially effective, but becomes ineffective close to the ridge where the ridge needs to be followed to its optimum. The necessary change in “search behavior” close to the ridge is difficult to diagnose, because the gradient towards the ridge does not flatten out.

- slope is 1:100

### 3.14 Different Powers Function

$$f_{14}(\mathbf{x}) = \sqrt{\sum_{i=1}^D |z_i|^{2+4\frac{i-1}{D-1}}} + f_{\text{opt}} \quad (14)$$

- $\mathbf{z} = \mathbf{R}(\mathbf{x} - \mathbf{x}^{\text{opt}})$

**Properties** Due to the different exponents the sensitivity relation of the  $z_i$ -variables continuously worsens when approaching the optimum.

## 4 Multi-modal functions with adequate global structure

### 4.15 Rastrigin Function

$$f_{15}(\mathbf{x}) = 10 \left( D - \sum_{i=1}^D \cos(2\pi z_i) \right) + \|\mathbf{z}\|^2 + f_{\text{opt}} \quad (15)$$

- $\mathbf{z} = \mathbf{R}\Lambda^{10}\mathbf{Q}T_{\text{asy}}^{0.2}(T_{\text{osz}}(\mathbf{R}(\mathbf{x} - \mathbf{x}^{\text{opt}})))$

**Properties** Prototypical highly multimodal function which has originally a very regular and symmetric structure for the placement of the optima. The transformations  $T_{\text{asy}}$  and  $T_{\text{osz}}$  alleviate the symmetry and regularity of the original Rastrigin function.

- non-separable less regular counterpart of  $f_3$
- roughly  $10^D$  local optima
- conditioning is about 10

### 4.16 Weierstrass Function

$$f_{16}(\mathbf{x}) = 10 \left( \frac{1}{D} \sum_{i=1}^D \sum_{k=0}^{11} 1/2^k \cos(2\pi 3^k (z_i + 1/2)) - f_0 \right)^3 + \frac{10}{D} f_{\text{pen}}(\mathbf{x}) + f_{\text{opt}} \quad (16)$$

- $\mathbf{z} = \mathbf{R}\Lambda^{1/100}\mathbf{Q}T_{\text{osz}}(\mathbf{R}(\mathbf{x} - \mathbf{x}^{\text{opt}}))$
- $f_0 = \sum_{k=0}^{11} 1/2^k \cos(2\pi 3^k 1/2)$

**Properties** Highly rugged and moderately repetitive landscape, where the global optimum is not unique.

- the term  $\sum_k 1/2^k \cos(2\pi 3^k \dots)$  introduces the ruggedness, where lower frequencies have a larger weight  $1/2^k$ .

#### 4.17 Schaffers F7 Function

$$f_{17}(\mathbf{x}) = \left( \frac{1}{D-1} \sum_{i=1}^{D-1} \sqrt{s_i} + \sqrt{s_i} \sin^2\left(50 s_i^{1/5}\right) \right)^2 + 10 f_{\text{pen}}(\mathbf{x}) + f_{\text{opt}} \quad (17)$$

- $\mathbf{z} = \Lambda^{10} \mathbf{Q} T_{\text{asy}}^{0.5}(\mathbf{R}(\mathbf{x} - \mathbf{x}^{\text{opt}}))$
- $s_i = \sqrt{z_i^2 + z_{i+1}^2}$  for  $i = 1, \dots, D$

**Properties** A highly multimodal function where frequency and amplitude of the modulation vary.

- conditioning is low

#### 4.18 Schaffers F7 Function, moderately ill-conditioned

$$f_{18}(\mathbf{x}) = \left( \frac{1}{D-1} \sum_{i=1}^{D-1} \sqrt{s_i} + \sqrt{s_i} \sin^2\left(50 s_i^{1/5}\right) \right)^2 + 10 f_{\text{pen}}(\mathbf{x}) + f_{\text{opt}} \quad (18)$$

- $\mathbf{z} = \Lambda^{1000} \mathbf{Q} T_{\text{asy}}^{0.5}(\mathbf{R}(\mathbf{x} - \mathbf{x}^{\text{opt}}))$
- $s_i = \sqrt{z_i^2 + z_{i+1}^2}$  for  $i = 1, \dots, D$

**Properties** Moderately ill-conditioned counterpart to  $f_{17}$

- conditioning of about 1000

#### 4.19 Composite Griewank-Rosenbrock Function F8F2

$$f_{19}(\mathbf{x}) = \frac{10}{D-1} \sum_{i=1}^{D-1} \left( \frac{s_i}{4000} - \cos(s_i) \right) + 10 + f_{\text{opt}} \quad (19)$$

- $\mathbf{z} = \max\left(1, \frac{\sqrt{D}}{8}\right) \mathbf{R}\mathbf{x} + 0.5$
- $s_i = 100(z_i^2 - z_{i+1})^2 + (z_i - 1)^2$  for  $i = 1, \dots, D$
- $\mathbf{z}^{\text{opt}} = \mathbf{1}$

**Properties** Resembling the Rosenbrock function in a highly multimodal way.

## 5 Multi-modal functions with weak global structure

### 5.20 Schwefel Function

$$f_{20}(\mathbf{x}) = -\frac{1}{D} \sum_{i=1}^D z_i \sin(\sqrt{|z_i|}) + 4.189828872724339 + 100f_{\text{pen}}(\mathbf{z}/100) + f_{\text{opt}} \quad (20)$$

- $\hat{\mathbf{x}} = 2 \times \mathbf{1}_-^+ \otimes \mathbf{x}$
- $\hat{z}_1 = \hat{x}_1$ ,  $\hat{z}_{i+1} = \hat{x}_{i+1} + 0.25 (\hat{x}_i - x_i^{\text{opt}})$  for  $i = 1, \dots, D-1$
- $\mathbf{z} = 100 (\Lambda^{10}(\hat{\mathbf{z}} - \mathbf{x}^{\text{opt}}) + \mathbf{x}^{\text{opt}})$
- $\mathbf{x}^{\text{opt}} = 4.2096874633/2 \mathbf{1}_-^+$ , where  $\mathbf{1}_-^+$  is the same realization as above

**Properties** The most prominent  $2^D$  minima are located comparatively close to the corners of the unpenalized search area.

- the penalization is essential, as otherwise more and better minima occur further away from the search space origin.

### 5.21 Gallagher's Gaussian 101-me Peaks Function

$$f_{21}(\mathbf{x}) = T_{\text{osz}} \left( 10 - \max_{i=1}^{101} w_i \exp \left( -\frac{1}{2D} (\mathbf{x} - \mathbf{y}_i)^T \mathbf{R}^T \mathbf{C}_i \mathbf{R} (\mathbf{x} - \mathbf{y}_i) \right) \right)^2 + f_{\text{pen}}(\mathbf{x}) + f_{\text{opt}} \quad (21)$$

- $w_i = \begin{cases} 1.1 + 8 \times \frac{i-2}{99} & \text{for } i = 2, \dots, 101 \\ 10 & \text{for } i = 1 \end{cases}$ , three optima have a value larger than 9
- $\mathbf{C}_i = \Lambda^{\alpha_i} / \alpha_i^{1/4}$  where  $\Lambda^{\alpha_i}$  is defined as usual (see Section 0.2), but with randomly permuted diagonal elements. For  $i = 2, \dots, 101$ ,  $\alpha_i$  is drawn uniformly randomly from the set  $\{1000^{2 \cdot \frac{j}{99}} \mid j = 0, \dots, 99\}$  without replacement, and  $\alpha_i = 1000$  for  $i = 1$ .
- the local optima  $\mathbf{y}_i$  are uniformly drawn from the domain  $[-4.9, 4.9]^D$  for  $i = 2, \dots, 101$  and  $\mathbf{y}_1 \in [-4, 4]^D$ . The global optimum is at  $\mathbf{x}^{\text{opt}} = \mathbf{y}_1$ .

**Properties** The function consists of 101 optima with position and height being unrelated and randomly chosen (different for each instantiation of the function).

- the conditioning around the global optimum is about 30

### 5.22 Gallagher's Gaussian 21-hi Peaks Function

$$f_{22}(\mathbf{x}) = T_{\text{osz}} \left( 10 - \max_{i=1}^{21} w_i \exp \left( -\frac{1}{2D} (\mathbf{x} - \mathbf{y}_i)^T \mathbf{R}^T \mathbf{C}_i \mathbf{R} (\mathbf{x} - \mathbf{y}_i) \right) \right)^2 + f_{\text{pen}}(\mathbf{x}) + f_{\text{opt}} \quad (22)$$

- $w_i = \begin{cases} 1.1 + 8 \times \frac{i-2}{19} & \text{for } i = 2, \dots, 21 \\ 10 & \text{for } i = 1 \end{cases}$ , two optima have a value larger than 9
- $\mathbf{C}_i = \Lambda^{\alpha_i} / \alpha_i^{1/4}$  where  $\Lambda^{\alpha_i}$  is defined as usual (see Section 0.2), but with randomly permuted diagonal elements. For  $i = 2, \dots, 21$ ,  $\alpha_i$  is drawn uniformly randomly from the set  $\{1000^{2 \cdot \frac{j}{19}} \mid j = 0, \dots, 19\}$  without replacement, and  $\alpha_i = 1000^2$  for  $i = 1$ .
- the local optima  $\mathbf{y}_i$  are uniformly drawn from the domain  $[-4.9, 4.9]^D$  for  $i = 2, \dots, 21$  and  $\mathbf{y}_1 \in [-4, 4]^D$ . The global optimum is at  $\mathbf{x}^{\text{opt}} = \mathbf{y}_1$ .

**Properties** The function consists of 21 optima with position and height being unrelated and randomly chosen (different for each instantiation of the function).

- the conditioning around the global optimum is about 1000

### 5.23 Katsuura Function

$$f_{23}(\mathbf{x}) = \frac{10}{D^2} \prod_{i=1}^D \left( 1 + i \sum_{j=1}^{32} \frac{|2^j z_i - [2^j z_i]|}{2^j} \right)^{10/D^{1.2}} - \frac{10}{D^2} + f_{\text{pen}}(\mathbf{x}) \quad (23)$$

- $\mathbf{z} = \mathbf{Q} \Lambda^{100} \mathbf{R}(\mathbf{x} - \mathbf{x}^{\text{opt}})$

**Properties** Highly rugged and highly repetitive function with more than  $10^D$  global optima

### 5.24 Lunacek bi-Rastrigin Function

$$f_{24}(\mathbf{x}) = \min \left( \sum_{i=1}^D (\hat{x}_i - \mu_0)^2, dD + s \sum_{i=1}^D (\hat{x}_i - \mu_1)^2 \right) + 10 \left( D - \sum_{i=1}^D \cos(2\pi z_i) \right) + 10^4 f_{\text{pen}}(\mathbf{x}) \quad (24)$$

- $\hat{\mathbf{x}} = 2 \text{sign}(\mathbf{x}^{\text{opt}}) \otimes \mathbf{x}$
- $\mathbf{z} = \mathbf{Q} \Lambda^{100} \mathbf{R}(\hat{\mathbf{x}} - \mu_0 \mathbf{1})$
- $\mu_0 = 2.5, \mu_1 = -\sqrt{\frac{\mu_0^2 - d}{s}}, s = 1 - \frac{1}{2\sqrt{D+20} - 8.2}, d = 1$
- $\mathbf{x}^{\text{opt}} = \mu_0 \mathbf{1}_+^+$

**Properties** Highly multimodal function with two funnels around  $\mu_0 \mathbf{1}_+^+$  and  $-\mu_1 \mathbf{1}_+^+$  being superimposed by the cosine. Presumably different approaches need to be used for “selecting the funnel” and for search the highly multimodal function “within” the funnel. The function was constructed to be deceptive for some evolutionary algorithms with large population size.

- the funnel of the local optimum at  $-\mu_1 \mathbf{1}_+^+$  has roughly 70% of the search space volume within  $[-5, 5]^D$ .

## Acknowledgments

The authors would like to thank Arnold Neumaier for his constructive comments.

## References

- [1] S. Finck, N. Hansen, R. Ros, and A. Auger. Real-parameter black-box optimization benchmarking 2009: Presentation of the noiseless functions. Technical Report 2009/01, Research Center PPE, 2009.



## APPENDIX

### A Function Properties

#### A.1 Deceptive Functions

All “deceptive” functions provide, beyond their deceptivity, a “structure” that can be exploited to solve them in a reasonable procedure. .

#### A.2 Ill-Conditioning

Ill-conditioning is a typical challenge in real-parameter optimization and, besides multimodality, probably the most common one. Conditioning of a function can be rigorously formalized in the case of convex quadratic functions,  $f(\mathbf{x}) = \frac{1}{2}\mathbf{x}^T\mathbf{H}\mathbf{x}$  where  $\mathbf{H}$  is a symmetric definite positive matrix, as the condition number of the Hessian matrix  $\mathbf{H}$ . Since contour lines associated to a convex quadratic function are ellipsoids, the condition number corresponds to the square root of the ratio between the largest axis of the ellipsoid and the shortest axis. For more general functions, conditioning loosely refers to the square of the ratio between the largest direction and smallest of a contour line. The testbed contains ill-conditioned functions with a typical conditioning of  $10^6$ . We believe this a realistic requirement, while we have seen practical problems with conditioning as large as  $10^{10}$ .

#### A.3 Regularity

Functions from simple formulas are often highly regular. We have used a non-linear transformation,  $T_{osz}$ , in order to introduce small, smooth but clearly visible irregularities. Furthermore, the testbed contains a few highly irregular functions.

#### A.4 Separability

In general, separable functions pose an essentially different search problem to solve, because the search process can be reduced to  $D$  one-dimensional search procedures. Consequently, non-separable problems must be considered much more difficult and most benchmark functions are designed being non-separable. The typical well-established technique to generate non-separable functions from separable ones is the application of a rotation matrix  $\mathcal{R}$ .

#### A.5 Symmetry

Stochastic search procedures often rely on Gaussian distributions to generate new solutions and it has been argued that symmetric benchmark functions could be in favor of these operators. To avoid a bias in favor of highly symmetric operators we have used a symmetry breaking transformation,  $T_{asy}$ . We have also included some highly asymmetric functions.

#### A.6 Target function value to reach

The typical target function value for all functions is  $f_{opt} + 10^{-8}$ . On many functions a value of  $f_{opt} + 1$  is not very difficult to reach, but the difficulty versus function value is not uniform for all functions. These properties are not intrinsic, that is  $f_{opt} + 10^{-8}$  is not intrinsically “very good”. The value mainly reflects a scalar multiplier in the function definition.



---

Centre de recherche INRIA Saclay – Île-de-France  
Parc Orsay Université - ZAC des Vignes  
4, rue Jacques Monod - 91893 Orsay Cedex (France)

Centre de recherche INRIA Bordeaux – Sud Ouest : Domaine Universitaire - 351, cours de la Libération - 33405 Talence Cedex  
Centre de recherche INRIA Grenoble – Rhône-Alpes : 655, avenue de l'Europe - 38334 Montbonnot Saint-Ismier  
Centre de recherche INRIA Lille – Nord Europe : Parc Scientifique de la Haute Borne - 40, avenue Halley - 59650 Villeneuve d'Ascq  
Centre de recherche INRIA Nancy – Grand Est : LORIA, Technopôle de Nancy-Brabois - Campus scientifique  
615, rue du Jardin Botanique - BP 101 - 54602 Villers-lès-Nancy Cedex  
Centre de recherche INRIA Paris – Rocquencourt : Domaine de Voluceau - Rocquencourt - BP 105 - 78153 Le Chesnay Cedex  
Centre de recherche INRIA Rennes – Bretagne Atlantique : IRISA, Campus universitaire de Beaulieu - 35042 Rennes Cedex  
Centre de recherche INRIA Sophia Antipolis – Méditerranée : 2004, route des Lucioles - BP 93 - 06902 Sophia Antipolis Cedex

---

Éditeur  
INRIA - Domaine de Voluceau - Rocquencourt, BP 105 - 78153 Le Chesnay Cedex (France)  
<http://www.inria.fr>  
ISSN 0249-6399